Available online at www.sciencedirect.com
SCIENCE DIRECT®
Conference of Global Chinese Scholars on Hydrodynamics

EFFECTS OF REYNOLDS STRESS ON FLOW NOISE FROM VORTEX/HYDROFOIL INTERACTIONS

Z. C. Zheng, Y. Xu
Department of Mechanical and Nuclear Engineering, Kansas State University, Manhattan, Kansas 66506, USA,
e-mail : zzheng@ksu.edu

ABSTRACT: Acoustic field generated by a single vortex approaching a hydrofoil is studied. A combined vortex/RANS simulation for the near–field unsteady vorticity is developed to include effects from RANS Reynolds stresses. The far-field acoustics is calculated using a vortex sound formula with the near-field vorticity as the source. The results show that at a higher incident angle when the RANS shows a substantial region with strong Reynolds stresses, there is a significant increase in the sound level due to enhanced unsteady vorticity in the shed vortices near the trailing edge.

KEY WORDS: hydroacoustics, vortex method, hydrofoil, vortex sound.

1. INTRODUCTION

Many hydroacoustic problems related to naval structures can be simplified or modeled as flow over a hydrofoil. These problems include flow around submarines and propellers. While the interested flow over a hydrofoil is turbulent most of the time, acoustic effects due to Reynolds stresses need to be considered, in addition to flow noise generated by vortex shedding from the sharp edge of the hydrofoil. In this study, in order to investigate effects of Reynolds stress resulting from Reynolds-averaged Navier-Stokes simulation (RANS), a new computational method that combines a vortex method with RANS has been introduced. The resultant vorticity near-field is then used as source terms in a formula for far-field acoustic field. The philosophy here is to take advantage of different techniques that are suitable for providing different information of turbulent flow for hydroacoustic predictions. Following this philosophy, the mean turbulent flow is simulated using robust RANS solvers. The mean flow, steady or unsteady, is low frequency in nature. This low-frequency component allows RANS models to be used in the mean flow simulation with proper physics. The perturbed, inviscid, higher frequency flow component is simulated using a vortex method. It is expected that the vortex method simulation adequately represent large unsteady vortex structures that are responsible for the far-field acoustics. The far-field acoustic signals are then predicted using expressions for vortex sound (e.g., Ref.~1 and 2) attributed to the rate of change of motion and strength of the vortices obtained by the vortex method.

Hardin and Pope[3], [4] and Morris et al. [5] developed algorithms that split instantaneous properties of the flow where the viscous mean flow is obtained from the Navier-Stokes equations and the acoustic radiation is obtained from the numerical solution of a system of perturbed inviscid Euler equations. The difference between the two is that for the mean flow, the former used incompressible flow

The present model differs from the above mentioned models in two major aspects. First, the present model is to combine the Euler-type Navier-Stokes simulation with the Lagrange-type vortex tracking method. While the Euler-type grid-based simulation is good at providing fast-converging solutions for low-frequency viscous flow, the Lagrange-type meshless method is cheaper to track the evolution of unsteady, non-dissipative vortical flow structures. Second, in both of the

Biography : Z. C. Zheng, Associate Professor, Tel: (785)532-5610, Fax: (785)532-7057; **Y. Xu**, Ph.D. student.

algorithms by Hardin and Pope and by Morris et al., the perturbed component is directly treated as the acoustic signal, and therefore compressible Euler simulation is necessary. In the present model, the perturbed vortex simulation is still treated as the near-field source. A separate far-field acoustic formula is used to extract the acoustic field, based on Lighthill's analogy that matches the near-field incompressible vortex flow to the far-field acoustic field, such as those in Ref.~1 and 2. In this sense, the present model can be viewed as a three-part splitting algorithm: the mean flow RANS simulation, the perturbed unsteady vortex method, and the far-field asymptotic vortex sound formulation.

Because the present model is based on incompressible flow models, it is suitable for simulating low Mach number hydroacoustic flow. Particularly, the present model fits best under the situation when vortex shedding from the sharp edges of hydrodynamic structures, such as hydrofoilds, is the primary sound source, because the proposed vortex tracking method naturally simulates the evolution of shed vortices.

2. Theoretical Explanations of the Combined Method

We use the vorticity transport equation for two-dimensional viscous incompressible flow to explain the concept. The equation can be expressed as

$$\frac{\partial \omega}{\partial t} + u_j \frac{\partial \omega}{\partial x_j} = \frac{1}{\mathrm{Re}} \frac{\partial^2 \omega}{\partial x_j \partial x_j} \tag{1}$$

Let

$$\omega = \Omega + \omega', \tag{2}$$

and

$$u_i = U_i + u_i' \tag{3}$$

where the flow variables are split into the mean flow part and the perturbed part. Substituting Eqs. (2) and (3) into Eq. (1) and rearranging, Eq. (1) becomes

$$\frac{\partial \omega'}{\partial t} + (U_j + u_j')\frac{\partial \omega'}{\partial x_j} = -S$$

$$- u_j' \frac{\partial \Omega}{\partial x_j} + \frac{1}{\mathrm{Re}} \frac{\partial^2 \omega'}{\partial x_j \partial x_j} \tag{4}$$

where

$$S = \frac{\partial \Omega}{\partial t} + U_j \frac{\partial \Omega}{\partial x_j} - \frac{1}{\mathrm{Re}} \frac{\partial^2 \Omega}{\partial x_j \partial x_j} \tag{5}$$

The mean flow source term, S, would yield terms of spatial derivatives of Reynolds stress in a RANS mean flow computation. Therefore it is zero for laminar flow. The last term in Eq. (4), the viscous term for the perturbed component, is neglected because the time averaged properties are the results of dissipative mechanics whereas the fluctuations are essentially inviscid. By neglecting the viscous effect on the perturbed component, Eq. (4) can be expressed in an equivalent Lagrangian formulation as

$$\frac{d\omega'}{dt}(\vec{\chi}, t) = -S(\vec{\chi}, t) - u_j'(\vec{\chi}, t)\frac{\partial \Omega}{\partial x_j}(\vec{\chi}, t) \tag{6}$$

and

$$\frac{d\vec{\chi}}{dt} = \vec{U} + \vec{u}' \tag{7}$$

where $\vec{\chi}$ prescribes the trajectory of a fluid element with vorticity ω'.By including $\vec{u}'$ in Eq. (7), the perturbed vortex flow is non-linear.

Equations (6) and (7) can be solved by a Lagrangian tracking method. In this method, the continuous vorticity field can be concentrated into a finite number of point vorticity particles for simulation purposes. The vorticity field, ω_i', has the representation

$$\omega'(\vec{\chi}, t) = \sum_{n=1}^{N} \Gamma_n \delta\left[\vec{x} - \vec{x}_n(t)\right] \tag{8}$$

where δ is the two-dimensional Dirac delta function, $\vec{x}_n$ are the locations of the N vortices, and the $\Gamma_{i,n}$ are their respective vector circulations. The circulation, which is actually the volumetric vorticity, is defined within a region of R_n such that

$$\Gamma_n = \int_{R_n} \omega' d\vec{x} \tag{9}$$

The region R_n can be meaningfully defined as the viscous region for each of the vorticity particles. When each of the vorticity particles is tracked, Eqs. (6) and (7) become

$$\frac{d\Gamma_n}{dt} = \Gamma_n \frac{\partial(U_i + u_i')}{\partial x_j} + \int_{R_n} (-S - u_j' \frac{\partial \Omega}{\partial x_j}) d\vec{x} \qquad (10)$$

$$\frac{d\vec{\chi}_n}{dt} = \vec{U} + \vec{u}_n' \qquad (11)$$

Hence, the perturbed flow field can be solved by using an ordinary differential equation set of Eqs. (10) and (11). The perturbed velocity field, $\vec{u}'$ is related to a stream function as

$$\vec{u}' = \nabla \Psi \qquad (12)$$

$$\nabla^2 \Psi = -\omega' \qquad (13)$$

Therefore the velocity $\vec{u}'$ can be solved using the Biot-Savart integrals. On the solid surface, the zero-normal velocity condition is enforced for the inviscid perturbed flow using the boundary element methods. The integral in the vortex core region in Eq. (10) depends on the vortex core model and the distribution of the integrand. Other details and theoretical background for vortex methods can be found in Ref. 6.

Although the recent development in vortex methods enables DNS type simulations using vortex methods, [7] the vortex method used here just needs to be accurate enough to provide acoustic sources, up to the level of flow physics and the range of frequencies of the interested hydroacoustic applications. Particularly, the Reynolds stress information is included which has been known to have significant influence on far-field acoustics. In a splitting scheme similar to Hardin's but with Reynolds stress effects, Shen and Sorensen[8] developed a direct acoustic simulation scheme to compute the case of a turbulent flow over an airfoil, where the source terms were solely determined by the mean flow Reynolds stress.

3. VORTEX PASSING A HYDROFOIL

In the following example, a vortex passing a symmetric Joukowski foil is considered. The chord length is used as the characteristic length of the problem and the thickness is 0.2. In this model problem, the mean flow is a steady flow generated by a uniform flow over a hydrofoil. There is a single vortex approaching to the hydrofoil which creates the perturbed flow, i.e., the vortex shedding at the trailing edge. The perturbed vortex flow is represented by a set of concentrated incompressible point vortices. At every time step, a new vortex is shed near the trailing edge of the foil.

Cases with incident angles of 5º and 15º arecompared to investigate the effect of Reynolds stress. The mean flow is computed using RANS simulation with the $k-\varepsilon$ model. Figure 1 shows the Reynolds stress term, S in Eq. (10), in two-dimensional flow at the two different incident angles. It can be seen that the Reynolds stress term is much stronger and has a larger influence region in the case of 15º.

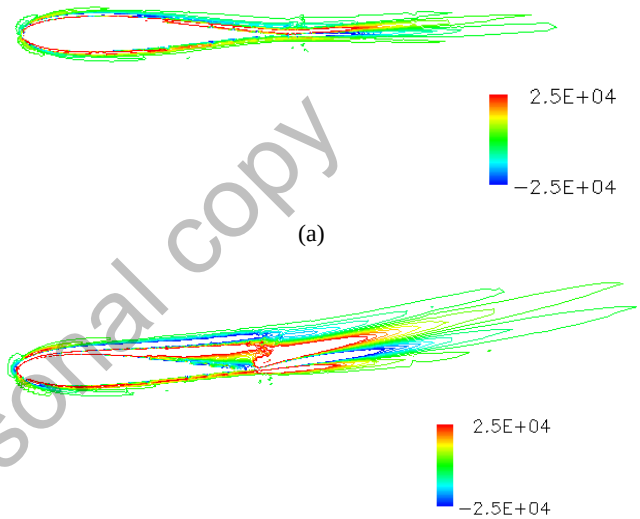

Fig. 1 Effect of incident angles on the Reynolds stress term. (a) 5º, (b) 15º.

Equations (10) and (11) are solved to track the strength and location of each vortex in the flow field. The time step size is determined by the highest resolvable frequency required in the problem. A two-dimensional relation between the near-field vortex dynamics and the far-field acoustic pressure fluctuation[9], [10] is then used to determine the acoustic properties:

$$\hat{p}_0 = -\frac{iM\omega}{4} H_1^{(2)}(\omega R)\left\{\sin\theta \cdot F\left[\sum_{n=1}^{N} \frac{d(\Gamma_n x_n)}{dt}\right] - \cos\theta \cdot F\left[\sum_{n=1}^{N} \frac{d(\Gamma_n y_n)}{dt}\right]\right\} \qquad (14)$$

where M is the Mach number based on the free-stream speed, R is the far-field distance,

(x_n, y_n) is the instantaneous location of the vortex Γ_n, $H_1^{(2)}$ is the Hankel function of the second kind of order one, and $F[\cdot]$ represents the Fourier transform for time.

Figure 2 is the far-field directivity of acoustic pressure. In the case of 15º the approaching vortex starts at (-1.5, -0.5), while in the cases of 5º the approaching vortex starts at (-1.5, -0.1). The reason that different starting points are selected for different incident angles is to obtain similar paths for the approaching vortex to pass by the hydrofoil, and therefore fair comparisons between different incident angle cases can be facilitated in terms of interactions between the approaching vortex and the hydrofoil. It can be seen in Fig. 2 that for the 5º cases, the Reynolds stress effect is not significant, because the Reynolds stress term shown in Fig. 1(a) has lower values and smaller influence regions. For the 15º cases, the Reynolds stress effect is very significant. When the Reynolds stress term is included, the pressure level is increased significantly, which agrees to the Reynolds-stress-term contours shown in Fig. 1(b) that have higher values and larger influence regions.

The dipole nature of the directivity is indicated in Eq. (14), because the acoustic pressure is related to the impulse of the vortex system. The change of vortex impulse generates dipole-type sources, as pointed out by Mohring[2]. The dipole-type directivity is also shown in Ref. 11, where no Reynolds stress effects are considered and the surface pressure on an airfoil is integrated to calculate the far-field noise. The effect of Reynolds stress on the magnitude of the far-field noise, as shown in Fig. 2, is dipole-type, although the Reynolds stress itself only produces quadrupole noise. In the vortex/hydrofoil interaction problem, the Reynolds stress influences the impulse of the vortex system which results in dipole-type noise. The influence of Reynolds stress on the surface pressure fluctuation, which can be a cause of the impulse change, also generates dipole noise. The surface-dipole effect is included in Eq. (14), which is equivalent to finding an adequate Green's function for the surface effect.

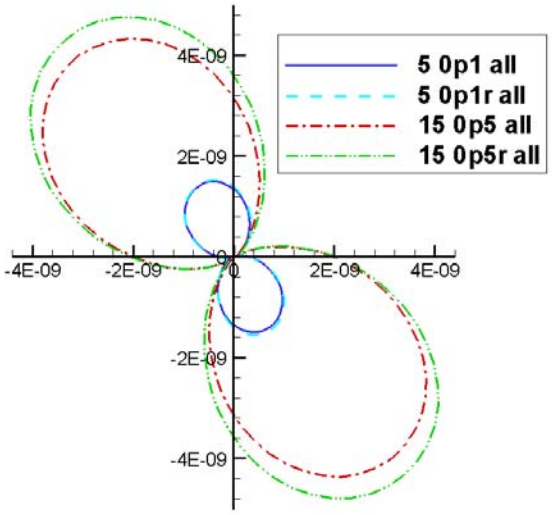

Fig. 2 Far-field acoustic pressure directivity (all vortices), where 5 0p1r means incident angle of 5 degree staring at (-1.5, -0.1) with Reynolds stress effects, 5 0p1 is the same case with Reynolds stress effects turned off. 150p5r means incident angle of 5 degree starting at (-1.5, -0.5) with Reynolds stress effects, and 150p5 is the same case with Reynolds stress effects turned off.

In order to find out the influence of Reynolds stress on the vortex dynamics, snapshots of vortex positions are plotted in Fig. 3 for the two 15º cases (with and without the Reynolds stress term). It can be seen although the overall major features of the two snap shots are similar, there is a significant difference in the length of the negative sign and positive sign vortices. The case with the Reynolds stress effect shows a longer negative vortex lines. We have tested whether the motion change (the dx_n/dt and dy_n/dt part in Eq. (14)) or the strength change (the $d\Gamma_n/dt$ part in in Eq. (14)) contributes more to the far-field noise, and found out that the motion change part is dominant. That means the Reynolds stress term, while directly changes the strength of the vortices as shown in Eq. (10), influences the motion of the vortices significantly that causes the significant change in the noise level.

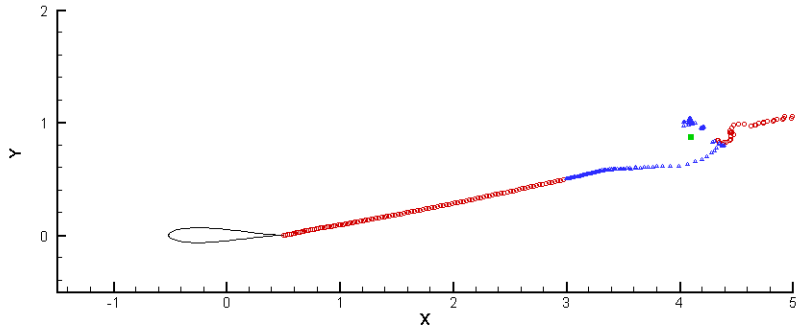

(a)

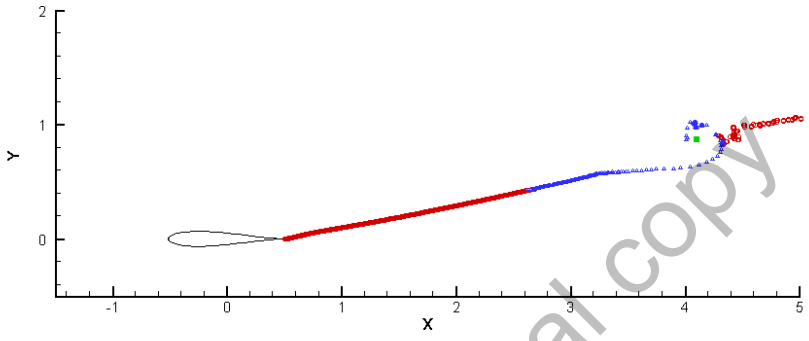

(b)

Fig. 3 Snap shots of the locations of vortices for the 15º cases. The red dots represent positive (counter clockwise) vortices, the blue deltas negative vortices, and the green square is the approaching vortex (positive). (a) without the Reynolds stress effect, (b) with the Reynolds stress effect.

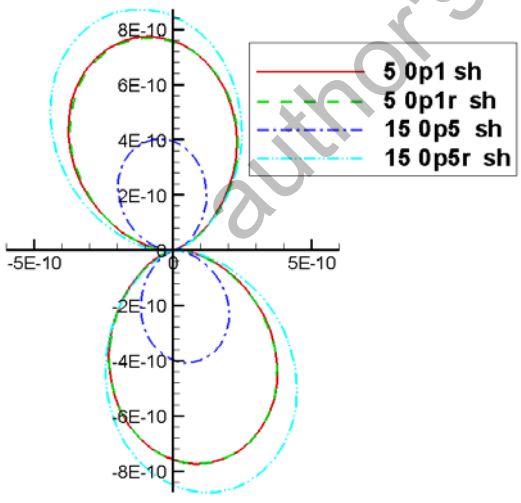

Fig. 4 Far-field acoustic pressure directivity (shed vortices).

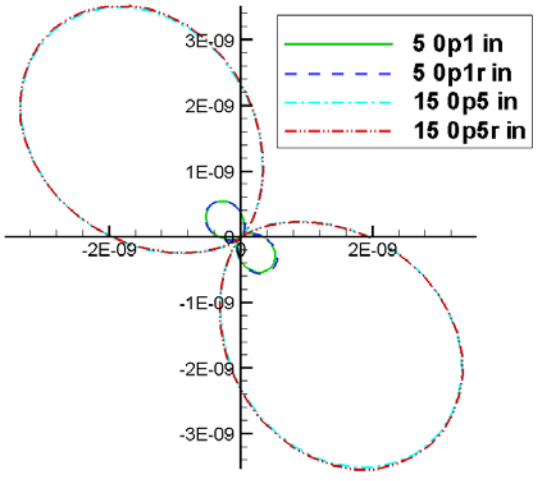

Fig. 5 Far-field acoustic pressure directivity (incoming vortex)

Since both the incoming vortex and the induced vortex shedding are responsible for the sound generation, we need to find out which part of the vortices are the dominant source and which part of the vortices that the Reynolds stresses influence the most. Figures 4 and 5 are plotted for that purpose. Figure 4 is the far-field pressure directivity from shed vortices only, and Fig. 5 is that from the incoming vortex only. In comparison to Fig. 2, which is the directivity for all the vortices, it can be seen in Fig. 5 that the major portion (about three-fourth) of noise is from the incoming vortex. The Reynolds stresses have little influence on this part of acoustics. When only is the incoming vortex concerned, the 15º cases have

stronger sound than the 5^o cases. The shed vortices are responsible for one-fourth of the overall sound. The Reynolds stresses, on the other hand, have significant effects in the 15^o cases on shed vortices in Fig. 4. When the Reynolds stress term is turned off, the 15^o case shows a lower acoustic pressure level than the 5^o cases. When the Reynolds-stress effect is included, the two 15^o cases show a significant difference. This difference is also translated into the directivity for all the vortices in Fig. 2. It makes sense that in the 15^o case the Reynolds stresses have more influences on the shed vortices, because the shed vortices have to pass through a region with strong Reynolds stress effects, a region shown in Fig.1.

4. CONCLUSION

A vortex/RANS combined method is used to calculate the vorticity field as the source region for the far-field acoustics generated by a vortex approaching a hydrofoil. It is shown that the Reynolds stress term included in the vorticity transport equation gives rise to the noise level through the unsteady flow field of shed vortices. This influence is significant when there is a relative large region with strong Reynolds stress effects. In the cases compared in this paper, the 5^o and 15^o cases, the 15^o case experiences a stronger Reynolds stress effect because there is a large and strong Reynolds stress region near the trailing edge in its RANS simulation. In the cases studied here, the Reynolds stresses have little effects on the sound generation from the incoming vortex.

REFERENCES

[1] Howe, M. S., Theory of Vortex Sound, Cambridge University Press, Cambridge, U. K., 2003.

[2] Mohring, W., On Vortex Sound at Low Mach Number, Journal of Fluid Mechanics, Vol. 85, 1978, pp. 685-691.

[3] Hardin, J. C., and Pope, D. S., An Acoustic/Viscous Splitting Technique for Computational Aeroacoustics, Theo. and Comp. Fluid Dynamics, Vol. 6, 1994, pp. 323-340.

[4] Hardin, J. C., and Pope, D. S., Sound Generation by Flow over a Two-Dimensional Cavity, AIAA Journal, Vol. 33, 1995, pp. 407-412.

[5] Morris, P. J., Long, L. N., Bangalore, A., and Wang, Q., A Parallel Three-Dimensional Computational Aeroacoustics Method Using Nonlinear Disturbance Equations, Vol. 133, 1997, pp. 56-74.

[6] Cottet, G.-H., and Koumoutsakos, P., Vortex Methods, Theory and Practice, Cambridge University Press, 2000.

[7] Cottet, G.-H., Michaux, B., Ossia, S., and Vanderlinden, G., A Comparison of Spectral and Vortex Methods in Three-Dimensional Incompressible Flows, Journal of Computational Physics, Vol. 175, 2002, pp. 1-11.

[8] Shen, W. Z., and Sorensen, J. N., Aeroacoustic Modeling of Turbulent Airoil Flows, Vol. 39, No. 6, 2001, pp. 1057-1064.

[9] Kao, H. C., Body-Vortex Interaction, Sound Generation, and Destructive Interference, AIAA Journal, Vol. 40, No. 4, 2002, pp. 652-660.

[10] Z. C. Zheng, Far-field Acoustic Pressure from a System of Discrete Vortices with Time-Varying Circulation, AIAA Paper 2005-3005, 11th AIAA/CEAS Aeroacoustics Conference, May 23-25, 2005, Monterey, CA.

[11] Guo, Y. P., Application of the Ffowcs Williams/Hawkings Equation to Two-Dimensional Problems, Journal of Fluid Mechanics, Vol. 403, 2000,pp. 201-221.